Published in final edited form as:

Cell Struct Funct. 2018 July 19; 43(2): 119–127. doi:10.1247/csf.18014.

Detailed analysis of the interaction of yeast COG complex

Midori Ishii[a,b], **Vladimir V. Lupashin**[c], and **Akihiko Nakano**[a,b]

[a]Live Cell Super-Resolution Imaging Research Team, RIKEN Center for Advanced Photonics, 2-1 Hirosawa, Wako, Saitama 351-0198, Japan

[b]Department of Biological Sciences, Graduate School of Science, The University of Tokyo, 7-3-1 Hongo, Bunkyo-ku, Tokyo 113-0033, Japan

[c]Department of Physiology and Biophysics, University of Arkansas for Medical Sciences, Little Rock, AR, USA

Abstract

The Golgi apparatus is a central station for protein trafficking in eukaryotic cells. A widely accepted model of protein transport within the Golgi apparatus is cisternal maturation. Each cisterna has specific resident proteins, which are thought to be maintained by COPI-mediated transport. However, the mechanisms underlying specific sorting of these Golgi-resident proteins remain elusive. To obtain a clue to understand the selective sorting of vesicles between the Golgi cisterenae, we investigated the molecular arrangements of the conserved oligomeric Golgi (COG) subunits in yeast cells. Mutations in COG subunits cause defects in Golgi trafficking and glycosylation of proteins and are causative of Congenital Disorders of Glycosylation (CDG) in humans. Interactions among COG subunits in cytosolic and membrane fractions were investigated by co-immunoprecipitation. Cytosolic COG subunits existed as octamers, whereas membrane-associated COG subunits formed a variety of subcomplexes. Relocation of individual COG subunits to mitochondria resulted in recruitment of only a limited number of other COG subunits to mitochondria. These results indicate that COG proteins function in the forms of a variety of subcomplexes and suggest that the COG complex does not comprise stable tethering without other interactors.

Keywords

The Golgi apparatus; COG complex; yeast; membrane trafficking; multi-subunit tethering complex

Introduction

It is essential for cellular organelles to maintain characteristic molecular compositions. Protein transport between single-membrane-bounded organelles is mostly mediated by membrane carriers, such as vesicles and tubules that bud from a donor membrane and fuse

Correspondence should be addressed to: Akihiko Nakano, Live Cell Super-Resolution Imaging Research Team, RIKEN Center for Advanced Photonics, 2-1 Hirosawa, Wako, Saitama 351-0198, Japan, nakano@riken.ac.jp, Phone: +81-48-467-9547, Fax: +81-48-462-4679.

with a target membrane. The transport of cargo molecules is regulated by sets of proteins such as SNAREs, small GTPases of Sar/Arf and Rab families, vesicle coat and tethering proteins (Bonifacino and Glick, 2004; Cai *et al.*, 2007). The Golgi apparatus functions as a central station of the membrane trafficking system in eukaryotic cells. It consists of flattened membrane-enclosed compartments, called cisternae, which are orderly differentiated in their functions and structures from cis to trans. Each cisterna has specific resident proteins such as glycosylation enzymes (Munro, 1998; Orlean, 2012). In the cisternal maturation model of the Golgi, the Golgi cisternae containing cargo progress and mature from cis to trans, while Golgi-resident proteins are recycled from later to earlier cisternae (Glick and Nakano, 2009; Nakano and Luini, 2010; Glick and Luini, 2011). To maintain the resident-protein localization to specific cisternae, their transport must be thoroughly regulated. Inhibition of COPI function results in the blockade of cisternal maturation (Papanikou *et al.*, 2015; Ishii *et al.*, 2016), indicating the essential role of COPI for maturation. Then, how do COPI vesicles selectively sort Golgi-resident proteins to their locations?

The COG complex belongs to the CATCHR (complexes associated with tethering containing helical rods) family multi-subunit tethering complex. The COG complex containing eight subunits (Cog1–8) is conserved from yeast to mammals and regulates early steps of the secretory pathway (Wuestehube *et al.*, 1996; VanRheenen *et al.*, 1998; VanRheenen *et al.*, 1999; Whyte and Munro, 2001; Suvorova *et al.*, 2002; Ungar *et al.*, 2002). The COG complex can be functionally and structurally separated into two subcomplexes, the lobe A (Cog1–4) and the lobe B (Cog5–8) (Fotso *et al.*, 2005; Oka *et al.*, 2005; Ungar *et al.*, 2005). In yeast, mutation or deletion of lobe A subunits causes severe growth defects, whereas deletion of lobe B subunits does not affect cell growth (Lees *et al.*, 2010). COG subunits directly interact with multiple Golgi SNARE proteins, COPI coat and Rab GTPases (Suvorova *et al.*, 2002; Willett *et al.*, 2013). Thus mutations in yeast COG subunits exhibit a variety of defects such as Golgi morphology, intra-Golgi and endosomal transport, and Golgi glycosylation enzyme activities (Whyte and Munro, 2001; Suvorova *et al.*, 2002; Bruinsma *et al.*, 2004; Fotso *et al.*, 2005). In studies of mammalian cells, COG subunits are present as independent sub-complexes on membranes (Willett *et al.*, 2016) and are shown to recruit different SNARE proteins and work as specific landmarks of vesicle tethering on the Golgi membrane (Willett *et al.*, 2013). Every subunit has been shown essential for the COG complex function in Golgi trafficking, though to varying extents (Bailey Blackburn *et al.*, 2016). Relocation of a lobe A subunit, COG4, to mitochondria recruited membranes bearing Golgi SNARE protein STX5 (Sed5 in yeast). A lobe B subunit, COG8, recruited membranes that carry TGN SNARE protein, STX16 (Tlg2 in yeast). The interaction between individual COG proteins and other Golgi transport machinery has also been investigated by pull-down and yeast two-hybrid methods (Suvorova *et al.*, 2002; Shestakova *et al.*, 2007). However, the details of in vivo interactions among COG subunits are not fully understood in yeast.

To understand the molecular arrangements of the COG subunits in vivo, we analyzed in detail the interactions among COG subunits in cytosolic and membrane fractions by co-immunoprecipitation in the present study. Both the lobe A and the lobe B subunits interacted with all other subunits in the cytosolic fraction, suggesting that cytosolic COG subunits exist as octamers. By contrast, membrane-associated COG subunits form a variety of subcomplexes. The results indicated complex features of inter-subunit interactions in yeast

cells. Further investigating interactions of COG proteins, one of each COG subunits were ectopically targeted to mitochondria membrane. Mitochondrial COG relocation experiments showed that exogenously expressed mitochondria-associated COG proteins were able to recruit other subunits, but could not outcompete the endogenous Golgi-associated COG complex.

Materials and Methods

Yeast strains and plasmids

Yeast strains, plasmids and primers used in this study are listed in Tables S1, S2 and S3, respectively. ADE2+ cells were made by integration with pRS402 (Brachmann *et al.*, 1998) digested by StuI into the ade2 site. The DNA fragment coding FIS1 was obtained from yeast genomic DNA by PCR with the primers (KpnI-FIS1-F and FIS1w/Stop-NotI-R), digested by KpnI and NotI and subcloned into the KpnI-NotI sites of pYES2 to produce pYES2-FIS1. The DNA fragment coding mCherry was obtained from pFA6a-mCherry-natNT2 (Kurokawa *et al.*, 2014) by PCR with the primers (BamHI-xFP_inpYES2_InFu-Fwd and xFP-BamH_inpYES2_InFu-Rev) and subcloned into KpnI digested pYES2-FIS1 by In-Fusion cloning (Takara Bio, Kusatsu, Shiga, Japan) to produce pYES2-mCherry-FIS1. DNA fragment coding COG2, COG3, COG4 and COG5 were obtained from yeast genomic DNA by PCR with the primers (HindIII-COG2-F, COG2w/oStop-KpnI-R for COG2, HindIII-COG3-F, Cog3w/oStop-KpnI-R for COG3, HindIII-COG4-F, COG4w/oStop-KpnI-R for COG4 and HindIII-COG5-F, COG5w/oStop-KpnI-R for COG5), digested by HindIII and KpnI and subcloned into the HindIII-KpnI sites of pYES2-mCherry-FIS1 to produce pYES2-COG2, 3, 4 and 5-mCherry-FIS1. The DNA fragment coding COG1, COG6, COG7 and COG8 were obtained from yeast genomic DNA by PCR with the primers (HindIII-COG1 in pYES2 InFu-Fwd, COG1w/oStop-KpnI in pYES2-mCh-FIS1 InFu-Rev for COG1, HindIII-COG6 in pYES2 InFu-Fwd, COG6w/oStop-KpnI in pYES2-mCh-FIS1 InFu-Rev for COG6, HindIII-COG7 in pYES2 InFu-Fwd, COG7w/oStop-KpnI in pYES2-mCh-FIS1 InFu-Rev for COG7 and HindIII-COG8 in pYES2 InFu-Fwd, COG8w/oStop-KpnI in pYES2-mCh-FIS1 InFu-Rev) and subcloned into HindIII and KpnI digested pYES2-mCherry-FIS1 by In-Fusion cloning to produce pYES2-COG1, 6, 7 and 8-mCherry-FIS1. pYES2-COG-mCherry-FIS1s were digested with BamHI to remove mCherry and self-ligated to produce pYES2-COG-FIS1s.

The DNA fragments of GAL1pr-COG4, 5, 6, 7 and 8-mCherry-FIS1-CYC1term were obtained from pYES2-COG4, 5, 6, 7 and 8-mCherry-FIS1 respectively by PCR with primers (SacII-GAL1p-F, CYC1term-SalI-R), digested by SacII and SalI and subcloned into SacII-SalI sites of pRS306 to produce pRS306-GAL1pr-COG4, 5, 6, 7, and 8-mCherry-FIS1-CYC1term. The DNA fragments of GAL1pr-COG1, 2 and 3-mCherry-FIS1-CYC1term were obtained from pYES2-COG1, 2 and 3-mCherry-FIS1 respectively by PCR with primers (SacII-GAL1p-F, CYC1t-SmaI-R), digested by SacII and SmaI and subcloned into SacII-SmaI sites to produce pRS306-GAL1pr-COG1, 2 and 3-mCherry-FIS1-CYC1term.

The DNA fragment coding COG1 and COG3 were obtained from yeast genomic DNA by PCR with primers (NotI-COG1-F, COG1w/Stop-XhoI-R for COG1 and NotI-COG3-F, COG3w/Stop-XhoI-R for COG3), digested by NotI and XhoI subcloned into the NotI-XhoI

sites of pYES2 to produce pYES2-COG1 and pYES2-COG3. The DNA fragment coding COG2 was obtained from yeast genomic DNA by PCR with primers (HindIII-COG2-F, COG2w/Stop-KpnI-R), digested by HindIII and KpnI and subcloned into HindIII-KpnI sites of pYES2 to produce pYES2-COG2. The DNA fragments coding COG4 was obtained from yeast genomic DNA by PCR with primers (HindIII-COG4-F, COG4w/Stop-XhoI-R), digested by HindIII and XhoI and subcloned into HindIII-XhoI sites of pYES2 to produce pYES2-COG4. The DNA fragments coding COG5, COG6, COG7 and COG8 were obtained from yeast genomic DNA by PCR with primers (BamHI-COG5-F, COG5w/Stop-SalI-R for COG5, BamHI-COG6-F, COG6w/Stop-SalI-R for COG6, BamHI-COG7-F, COG7w/Stop-SalI-R for COG7 and BamHI-COG8-F, COG8w/Stop-SalI-R for COG8), digested by BamHI and SalI and subcloned into BamHI-XhoI sites of pYES2 to produce pYES2-COG5, pYES2-COG6, pYES2-COG7 and pYES2-COG8.

Gene disruptions of COG subunits (YPH499 background) were constructed by a PCR-based methods using cog5, 6, 7 and 8::kanMX6 (BY4741, Invitrogen, Thermo Fisher Scientific, Waltham, MA, USA) genome DNA as templates with primers (COG5upATG200b-F, COG5downStop200b-R for cog5Δ, COG6upATG100b-F, COG6downStop100b-R for cog6Δ, COG7upATG200b-F, COG7downStop200b-R for cog7Δ and COG8upATG100b-F, COG8downStop100b-R for cog8Δ).

pRS306-GAL1p-COG1-mCherry-FIS1, pRS306-GAL1p-COG2-mCherry- FIS1, pRS306-GAL1p-COG3-mCherry-FIS1, pRS306-GAL1p-COG4-mCherry-FIS1, pRS306-GAL1p-COG6-mCherry-FIS1 and pRS306-GAL1p-COG8-mCherry-FIS1 were digested by NdeI and integrated into the ura3 site of the yeast genome. pRS306-GAL1p-COG5-mCherry-FIS1 was digested by EcoRV and integrated into the ura3 site of the yeast genome. pRS306-GAL1p-COG7-mCherry-FIS1 was digested by BstBI and integrated into the ura3 site of the yeast genome.

pRS316-GFP-SED5 or pRS316-GFP-GOS1 were digested by PvuI and transformed with EcoRI digested pRS314.

Microscopy

Fluorescence microscopy was performed by super-resolution confocal microscopy (SCLIM) with a UPlanSApo 100 × NA 1.4 oil objective lens (Olympus, Tokyo, Japan), a high-speed spinning-disk confocal scanner (Yokogawa Electric, ,Tokyo, Japan), a custom-made spectroscopic unit, image intensifiers (Hamamatsu Photonics, Hamamatsu, Japan) with a custom-made cooling system, and two EM-CCD cameras (Hamamatsu Photonics) (Kurokawa *et al.*, 2013). For microscopic observation, all strains were grown in selective medium (0.67% yeast nitrogen base without amino acids and 2% glucose) with appropriate supplements. For imaging of COG-mCherry-Fis1 cells, 42 optical slices spaces 0.1 μm apart were collected. Maximum intensity projection was conducted by z project of Fiji plugin Max Intensity (Schindelin *et al.*, 2012).

COG-GFP Pull Down

Endogenous COG1, 3, 5 and 6 were tagged with GFP at C-termini. Cells were grown at 30˚C in YPD medium. 200 OD600 unit cells were harvested, resuspended in 0.1 M Tris-HCl

(pH9.4)/ 10 mM DTT, incubated at 30˚C for 10 minutes, harvested, resuspend in 50 mM HEPES pH7.2/ 0.8 M mannitol/ 20 μL zymolyase, and spheroplasted for 1 h at 30˚C. Spheroplasts were harvested by centrifugation at 2,000 × g 5 minutes and washed with 50 mM HEPES pH7.2/ 0.8 M mannitol. The pellet was resuspend in YPD with 0.8 M mannitol and incubated for 90 minutes at 30˚C. Cells were harvested by centrifugation at 2,000 × g for 5 minutes, washed with 50 mM HEPES pH7.2/ 0.8 M mannitol. Cells were resuspended 1 mL of IP buffer [150 mM NaCl/ 50 mM Tris (pH7.4)/ 7 μL/mL Halt Protease Inhibitor Cocktail EDTA free (Thermo Fisher)/ 1 mM PMSF] and homogenized by dounce homogenizer. Total cell lysates were centrifuged at 2,000 × g for 5 minutes at 4˚C to remove debris. Supernatants were separated into supernatant (cytosol) and pellet (membrane) fraction by ultracentrifugation at 100,000 × g for 1 h at 4˚C in a Beckman Optima MAX-XP Ultracentrifuge (TLA 55 rotor). Pellet was resuspended in 500 μL of IP buffer containing 1% Triton X-100, incubated on ice for 30 minutes and centrifuged at 10,000 × g for 5 minutes at 4˚C. Supernatant was used as membrane fraction (P100) for the following immunoprecipitation analysis. 500 μL of supernatant (S100, cytosol fraction) was solubilized with Triton X-100 (final concentration 1%) on ice for 30 minutes. 1 μL of anti-GFP antibody (mouse monoclonal, 3E6, Thermo Fisher) was added to both membrane and cytosol fractions and incubated on ice in a cold room overnight. 60 μL of 30% Protein G beads (Protein G-Agarose, Roche Diagnostics, Mannheim, Germany) was added to each tube and incubated with gentle mixing in a cold room for 2 h. Beads were then washed four times with PBS containing 0.05% Triton. Samples were eluted in 2× Laemmli sample buffer (Bio-Rad, Hercules, California, USA) and heated for 5 minutes at 95˚C to elute the bound proteins.

mCherry beads Immunoprecipitation

Cells were grown at 30˚C in selective medium with 2% galactose overnight. 200 OD600 unit cells were harvested, incubated at 30˚C for 10 minutes in 0.1 M Tris-HCl (pH9.4)/ 10 mM DTT, harvested, resuspend in 50 mM HEPES pH7.2/ 0.8 M mannitol/ 20 μL zymolyase, and spheroplasted for 1 h at 30˚C. Spheroplasts were harvested by centrifugation at 2,000 × g for 5 minutes. Spheroplasts were resuspend 1 mL of IP buffer and homogenized by dounce homogenizer. Total cell lysates were centrifuged at 2,000 × g for 5 minutes at 4˚C to remove debris. Triton X-100 (final concentration 1%) was added to supernatant and incubated on ice to solubilize. 60 μL of 50% mCherry-Nanobody beads (LaM4.2-His beads) (Fridy *et al.*, 2014) was added and incubated with gentle mixing at room temperature for 1.5 h. Beads were then washed four times with PBS containing 0.05% Triton. Samples were eluted in 2× Laemmli sample buffer (Bio-Rad) and heated for 5 minutes at 95˚C to elute the bound proteins.

Western blotting—Samples were analyzed by SDS/PAGE, followed by Western blotting with primary antibody anti-GFP (1: 1000, B34, COVANCE, Princeton, New Jersey, USA), anti-COG (anti-COG1, anti-COG3–6, anti-COG8, 1: 1000 and anti-COG2, 1: 250) (Fotso *et al.*, 2005), anti-mCherry (1: 500, rabbit polyclonal, Lupashin Lab). Bands were visualized by appropriate secondary antibodies conjugated with IRDye 680 or IRDye 800 dyes (LI-COR Biosciences, Lincoln, Nebraska, USA). Bands intensities were calculated by analysis tool of Image Studio Lite (LI-COR).

Results

COG-GFP immunoprecipitation

To investigate the in vivo interaction among yeast COG subunits in the cytosol and on the membrane, cells expressing GFP-tagged COG proteins were subjected to immunoprecipitation by the anti-GFP antibody. The immunoprecipitates were analyzed for the interaction with other subunits by Western blotting using antibodies against the individual COG subunits. GFP-tagged COG cells grew as wild type cells, indicating GFP-fusion COG proteins are functional. Cell lysates were separated into cytosolic (S100) and membrane (P100) fractions by centrifugation at 100,000 × g. COG proteins were found in both cytosolic and membrane fractions as described previously (Suvorova *et al.*, 2002). In the cytosolic fraction, all the eight subunits were co-immunoprecipitated with Cog1, Cog3, Cog5 and Cog6-GFP, confirming that all eight subunits were stably associated in a COG1–8 octameric complex in the cytosol fraction (Fig.1). On the other hand, COG subunits showed different interaction patterns in the membrane fraction. Cog1 co-immunoprecipitated both the lobe A (Cog1–4) and the lobe B (Cog5–8) subunits. Cog3 co-immunoprecipitated mainly the lobe A (Cog1–4) subunits. Cog5 did not show strong interactions with other subunits, whereas Cog6 interacted strongly with Cog8 (Fig. 1). These co-immunoprecipitation data suggest that membrane-associated COG subunits exist in the forms of subcomplexes; lobe A and lobe B. These results are consistent with the observation of HeLa cells, which showed that complete COG1–8 octamers were formed in the cytosolic fraction but a combination of octamers and subcomplexes were present in the membrane fraction (Willett *et al.*, 2016). Probably COG subunits strongly interact with each other in the cytosolic fraction but weakly in the membrane fraction. In other words, the COG complex may tend to dissociate into subcomplexes when they bind to the membrane or to membrane-associated protein partners.

Ectopic targeting of COG subunits to mitochondria

To determine the role of COG subunits in vesicle targeting, we developed constructs in a way that one of the COG subunits would be ectopically tethered to the mitochondrial outer membrane (Willett *et al.*, 2013). The mitochondrial protein Fis1 integrates its C-terminal transmembrane domain into the mitochondria outer membrane and exposes its N-terminus to cytosol (Mozdy *et al.*, 2000). The C-terminus of each of the eight individual COG subunits was fused to mCherry-Fis1 (COG-mCherry-Fis1 collectively, Fig. 2A). Expression of COG-mCherry-Fis1 fusion proteins was placed under control of the GAL1 promoter (strongly induced in a galactose-containing medium and repressed in a glucose-containing medium).

First, the growth of COG-mCherry-Fis1 or COG-Fis1 cells was examined on galactose-containing plates. As shown in Figure 2, neither the overexpression of untagged COG subunits by 2μ multicopy plasmids nor the COG-mCherry-Fis1 expression by chromosomal integration plasmids showed growth defects. By contrast, the overexpression of COG-mCherry-Fis1 by 2μ multicopy plasmids caused marked growth defects for the cases of Cog3, 4, 5 and 6. This indicates that overexpression of some specific COG subunits on the outer mitochondrial membrane is deleterious to cells. Interestingly, Western blotting with anti-mCherry or anti-Cog4 antibodies did not detect a band corresponding to Cog4-

mCherry-Fis1 either for integration or multicopy plasmid constructs (Fig S1), indicating that the expression of the full-length Cog4-mCherry-Fis1 protein was toxic and the cells kept the amount of proteins below the detection limit (see Fig. 2). COG-mCherry-Fis1 protein was confirmed to colocalize with a GFP-tagged mitochondria marker protein, Cit1 (Fig. S2).

COG subunits mislocalized to mitochondria recruit other COG subunits

Using mitochondria-localizing COG-mCherry-Fis1, we examined the recruitment of other COG subunits. For the subsequent analysis, we used the cells that expressed COG-mCherry-Fis1 by the integration plasmid, because they showed no growth defect. First the interaction among COG subunits was analyzed by co-immunoprecipitation. COG-mCherry-Fis1 was immunoprecipitated using mCherry-Nanobody (LaM4.2)-conjugated beads (Fridy *et al.*, 2014) and analyzed for interacting proteins by Western blotting with anti-COG antibodies.

Mitochondrially-mislocalized subunits of the lobe A, Cog1 and Cog3, co-immunoprecipited other subunits of both the lobe A and the lobe B (Fig. 3). The mislocalized lobe B subunit, Cog5-mCherry-Fis1, recruited other lobe B subunits and Cog4. The mislocalized Cog6-mCherry-Fis1 recruited other subunits of both the lobe A and the lobe B. The mislocalized Cog8-mCherry-Fis1 did not show appreciable interaction with other subunits, indicating that C-terminal tag may interfere with efficient incorporation of COG8 in the COG complex. In a previous study, Cog1 was shown to be important for recruiting the lobe B subunits (Fotso *et al.*, 2005). Here we showed that not only Cog1 but also Cog3 and Cog6 have the ability to recruit other subunits of both the lobe A and the lobe B.

The COG complex alone is insufficient to recruit Golgi derived vesicles

It has been shown that COG proteins interact with Golgi SNARE proteins, Sed5, Ykt6, Gos1 and Sed22 in yeast cells (Suvorova *et al.*, 2002). In mammalian cells, mislocalized COG4 and COG8 proteins are reported to recruit vesicles including Golgi and TGN SNARE proteins (Willett *et al.*, 2013). We examined localization of COG and SNARE proteins in cells expressing chromosomally-integrated COG-mCherry-Fis1. Cells were observed at 3 h after induction, under which condition mitochondria did not show abnormal morphology. As shown in Figure 4, Golgi SNAREs, Sed5 and Gos1 and TGN SNAREs, Tlg1 and Tlg2 were not recruited to Cog3 or Cog6. This result suggests that the tested mislocalized COG subunits are unable to fulfill full tethering activities of COG subunits. Long time induction (more than 6 h) of COG-mCherry-Fis1 often caused aggregation of mitochondria, however we could not observe SNARE mislocalizations even under this condition. This suggests that COG-mCherry-Fis1 could not stably recruit the Golgi derived vesicles to mitochondria. Alternatively, this level of overexpression was not sufficient to change fractionation profiles of the bulk of Golgi proteins. From these results, unfortunately, it remains elusive whether the individual COG subunit has the ability to recruit or keep tethering vesicles to the membrane. If not, other interactors, in addition to COG subunits themselves, might be needed for this function.

Discussion

The COG complex has been characterized as the peripheral protein complex that functions in the tethering of Golgi derived vesicles. Studies of yeast and mammalian cells have shown that the COG complex directly interacts with the Golgi SNARE complexes (Suvorova *et al.*, 2002; Shestakova *et al.*, 2007). In mammalian cells, COG4 and COG8 are reported to recruit different SNARE proteins and form different vesicle tethering platforms (Willett *et al.*, 2013). We hypothesized that the COG subunits of yeast cells also play roles as specific landmarks for different vesicles, and mediate specific intra-Golgi vesicle transport. In this study, we first analyzed interactions among the COG subunits in cytosol and on the membrane. COG subunits form a stable octameric complex in cytosol, whereas they form not only octamers but also various subcomplexes in the membrane fraction. Considering its function as a tethering complex, the cytosolic COG complex may not be fully active and the COG subunits that associate with each other in a variety of forms on the membrane should work as tethers. It is consistent with the result on mammalian cells that most of cytosolic COG subunits exist as octomers and membrane-associated COG proteins exist as smaller subcomplexes (Willett *et al.*, 2013; Willett *et al.*, 2016). Whereas the quadruple lobe B mutant yeast cells (Δcog5 Δcog6 Δcog7 Δcog8) grow normally like wild-type cells in the laboratory condition (Lees *et al.*, 2010), the mutations in lobe B subunits in human cause congenital disorders of glycosylation (CDG) diseases (Freeze and Ng, 2011). The roles of lobe B proteins might be different between species. Our result that COG proteins form multiple forms of subcomplexes on the membrane suggests that octamers and smaller subcomplexes play different roles on the membrane. Deciphering the different roles of the octameric complex and subcomplexes will need further investigations.

To further understand the roles of COG subunits, mitochondrial targeting assays have been employed (Sengupta *et al.*, 2009; Willett *et al.*, 2013; Luo *et al.*, 2014; Willett *et al.*, 2016). We used this method because direct vesicle sorting from the Golgi apparatus to the mitochondria is not known and the mislocalization of secretory machineries to mitochondria would separate them from the normal secretory pathway. This type of assay worked well in mammalian cells, in which mislocalized COG subunits specifically recruit vesicles containing SNARE proteins (Willett *et al.*, 2013) and in yeast cells, mislocalization of the CATCHR family tethering complex, exocyst subunit Sec3, recruited secretory vesicles (Luo *et al.*, 2014). We expected that ectopic targeting of specific COG subunits to mitochondria would give us some information about the specific vesicle tethering mechanism of the COG complex. It was unclear at this point whether the growth defects were due to relocation of the COG complex or they recruited unknown essential proteins to mitochondria. Importantly, overexpression of mitochondrial-targeted COG4 was very toxic in yeast cell, suggesting that potential recruitment of Sed5-containing membranes to mitochondria was interfering with normal yeast cell growth. Cog1, 3 and 6 recruited both lobe A and lobe B subunits, indicating that they are able to form a platform to assemble the octameric COG complex. If mitochondria-localized COGs were indeed unable to recruit vesicles, it would suggest that the COG complex interacts with other components for a short period of time and COG itself cannot maintain stable interactions with the vesicles. Recently, Anderson *et al.* (2017) reported that the mammalian CASP homolog, Coy1, interact with both COG

proteins and Golgi SNARE proteins (Anderson *et al.*, 2017). Further studies on interactors of the COG complex would provide better understanding of intra-Golgi trafficking.

Supplementary Material

Refer to Web version on PubMed Central for supplementary material.

Acknowledgements

This work was supported by Grants-in-Aid for Scientific Research from the Ministry of Education, Culture, Sports, Science, and Technology of Japan under grant [grant numbers JP25221103 to A.N] and by RIKEN President's Fund "4D measurements for Multilayered Cellular Dynamics" to A.N. M.I. was a Research Fellow of Japan Society for the Promotion of Science (JSPS) and was supported by a Grant-in-Aid for JSPS fellows under grant [grant number JP25221103]. VL was supported by the NIH grants under grant GM083144 and U54 GM105814.

We thank the Advanced Leading Graduate Course for Photon Science of The University of Tokyo for the support on this joint research.

Abbreviations:

CATCHR	complexes associated with tethering containing helical rods
COG	complex, conserved oligomeric Golgi complex
COPI	coat protein complex I
TGN	trans-Golgi network

References

Anderson NS, Mukherjee I, Bentivoglio CM and Barlowe C 2017 The golgin protein Coy1 functions in intra- Golgi retrograde transport and interacts with the COG complex and Golgi SNAREs. Mol. Biol. Cell, 28: 2686–2700.

Bailey Blackburn J, Pokrovskaya I, Fisher P, Ungar D and Lupashin VV 2016 COG Complex Complexities: Detailed Characterization of a Complete Set of HEK293T Cells Lacking Individual COG Subunits. Front. Cell Dev. Biol, 4: 23. [PubMed: 27066481]

Bonifacino JS and Glick BS 2004 The mechanisms of vesicle budding and fusion. Cell, 116: 153–166. [PubMed: 14744428]

Brachmann CB, Davies A, Cost GJ, Caputo E, Li J, Hieter P and Boeke JD 1998 Designer deletion strains derived from Saccharomyces cerevisiae S288C: a useful set of strains and plasmids for PCR-mediated gene disruption and other applications. Yeast, 14: 115–132. [PubMed: 9483801]

Bruinsma P, Spelbrink RG and Nothwehr SF 2004 Retrograde transport of the mannosyltransferase Och1p to the early Golgi requires a component of the COG transport complex. J. Biol. Chem, 279: 39814–39823. [PubMed: 15229219]

Cai H, Reinisch K and Ferro-Novick S 2007 Coats, tethers, Rabs, and SNAREs work together to mediate the intracellular destination of a transport vesicle. Dev. Cell, 12: 671–682. [PubMed: 17488620]

Fotso P, Koryakina Y, Pavliv O, Tsiomenko AB and Lupashin VV 2005 Cog1p plays a central role in the organization of the yeast conserved oligomeric Golgi complex. J. Biol. Chem, 280: 27613–27623. [PubMed: 15932880]

Freeze HH and Ng BG 2011 Golgi glycosylation and human inherited diseases. Cold Spring Harb Perspect Biol, 3: a005371. [PubMed: 21709180]

Fridy PC, Li Y, Keegan S, Thompson MK, Nudelman I, Scheid JF, Oeffinger M, Nussenzweig MC, Fenyo D, Chait BT and Rout MP 2014 A robust pipeline for rapid production of versatile nanobody repertoires. Nat. Methods, 11: 1253–1260. [PubMed: 25362362]

Glick BS and Luini A 2011 Models for Golgi traffic: a critical assessment. Cold Spring Harb Perspect Biol, 3: a005215. [PubMed: 21875986]

Glick BS and Nakano A 2009 Membrane traffic within the Golgi apparatus. Annu. Rev. Cell. Dev. Biol, 25: 113–132. [PubMed: 19575639]

Ishii M, Suda Y, Kurokawa K and Nakano A 2016 COPI is essential for Golgi cisternal maturation and dynamics. J. Cell Sci, 129: 3251–3261. [PubMed: 27445311]

Kurokawa K, Ishii M, Suda Y, Ichihara A and Nakano A 2013 Live cell visualization of Golgi membrane dynamics by super-resolution confocal live imaging microscopy. Methods in cell biology, 118: 235–242. [PubMed: 24295310]

Kurokawa K, Okamoto M and Nakano A 2014 Contact of cis-Golgi with ER exit sites executes cargo capture and delivery from the ER. Nat Commun, 5: 3653. [PubMed: 24728174]

Lees JA, Yip CK, Walz T and Hughson FM 2010 Molecular organization of the COG vesicle tethering complex. Nat. Struct. Mol. Biol, 17: 1292–1297. [PubMed: 20972446]

Luo G, Zhang J and Guo W 2014 The role of Sec3p in secretory vesicle targeting and exocyst complex assembly. Mol. Biol. Cell, 25: 3813–3822. [PubMed: 25232005]

Mozdy AD, McCaffery JM and Shaw JM 2000 Dnm1p GTPase-mediated mitochondrial fission is a multi-step process requiring the novel integral membrane component Fis1p. J. Cell Biol, 151: 367–380. [PubMed: 11038183]

Munro S 1998 Localization of proteins to the Golgi apparatus. Trends Cell Biol, 8: 11–15. [PubMed: 9695801]

Nakano A and Luini A 2010 Passage through the Golgi. Curr. Opin. Cell Biol, 22: 471–478. [PubMed: 20605430]

Oka T, Vasile E, Penman M, Novina CD, Dykxhoorn DM, Ungar D, Hughson FM and Krieger M 2005 Genetic analysis of the subunit organization and function of the conserved oligomeric golgi (COG) complex: studies of COG5- and COG7-deficient mammalian cells. J. Biol. Chem, 280: 32736–32745. [PubMed: 16051600]

Orlean P 2012 Architecture and biosynthesis of the Saccharomyces cerevisiae cell wall. Genetics, 192: 775–818. [PubMed: 23135325]

Papanikou E, Day KJ, Austin J and Glick BS 2015 COPI selectively drives maturation of the early Golgi. Elife, 4.

Schindelin J, Arganda-Carreras I, Frise E, Kaynig V, Longair M, Pietzsch T, Preibisch S, Rueden C, Saalfeld S, Schmid B, Tinevez JY, White DJ, Hartenstein V, Eliceiri K, Tomancak P and Cardona A 2012 Fiji: an open-source platform for biological-image analysis. Nat. Methods, 9: 676–682. [PubMed: 22743772]

Sengupta D, Truschel S, Bachert C and Linstedt AD 2009 Organelle tethering by a homotypic PDZ interaction underlies formation of the Golgi membrane network. J. Cell Biol, 186: 41–55. [PubMed: 19581411]

Shestakova A, Suvorova E, Pavliv O, Khaidakova G and Lupashin V 2007 Interaction of the conserved oligomeric Golgi complex with t-SNARE Syntaxin5a/Sed5 enhances intra-Golgi SNARE complex stability. J. Cell Biol, 179: 1179–1192. [PubMed: 18086915]

Suvorova ES, Duden R and Lupashin VV 2002 The Sec34/Sec35p complex, a Ypt1p effector required for retrograde intra-Golgi trafficking, interacts with Golgi SNAREs and COPI vesicle coat proteins. J. Cell Biol, 157: 631–643. [PubMed: 12011112]

Ungar D, Oka T, Brittle EE, Vasile E, Lupashin VV, Chatterton JE, Heuser JE, Krieger M and Waters MG 2002 Characterization of a mammalian Golgi-localized protein complex, COG, that is required for normal Golgi morphology and function. J. Cell Biol, 157: 405–415. [PubMed: 11980916]

Ungar D, Oka T, Vasile E, Krieger M and Hughson FM 2005 Subunit architecture of the conserved oligomeric Golgi complex. J. Biol. Chem, 280: 32729–32735. [PubMed: 16020545]

VanRheenen SM, Cao X, Lupashin VV, Barlowe C and Waters MG 1998 Sec35p, a novel peripheral membrane protein, is required for ER to Golgi vesicle docking. J. Cell Biol, 141: 1107–1119. [PubMed: 9606204]

VanRheenen SM, Cao X, Sapperstein SK, Chiang EC, Lupashin VV, Barlowe C and Waters MG 1999 Sec34p, a protein required for vesicle tethering to the yeast Golgi apparatus, is in a complex with Sec35p. J. Cell Biol, 147: 729–742. [PubMed: 10562277]

Whyte JR and Munro S 2001 The Sec34/35 Golgi transport complex is related to the exocyst, defining a family of complexes involved in multiple steps of membrane traffic. Dev. Cell, 1: 527–537. [PubMed: 11703943]

Willett R, Blackburn JB, Climer L, Pokrovskaya I, Kudlyk T, Wang W and Lupashin V 2016 COG lobe B sub-complex engages v-SNARE GS15 and functions via regulated interaction with lobe A sub-complex. Sci Rep, 6: 29139. [PubMed: 27385402]

Willett R, Kudlyk T, Pokrovskaya I, Schonherr R, Ungar D, Duden R and Lupashin V 2013 COG complexes form spatial landmarks for distinct SNARE complexes. Nat Commun, 4: 1553. [PubMed: 23462996]

Wuestehube LJ, Duden R, Eun A, Hamamoto S, Korn P, Ram R and Schekman R 1996 New mutants of Saccharomyces cerevisiae affected in the transport of proteins from the endoplasmic reticulum to the Golgi complex. Genetics, 142: 393–406. [PubMed: 8852839]

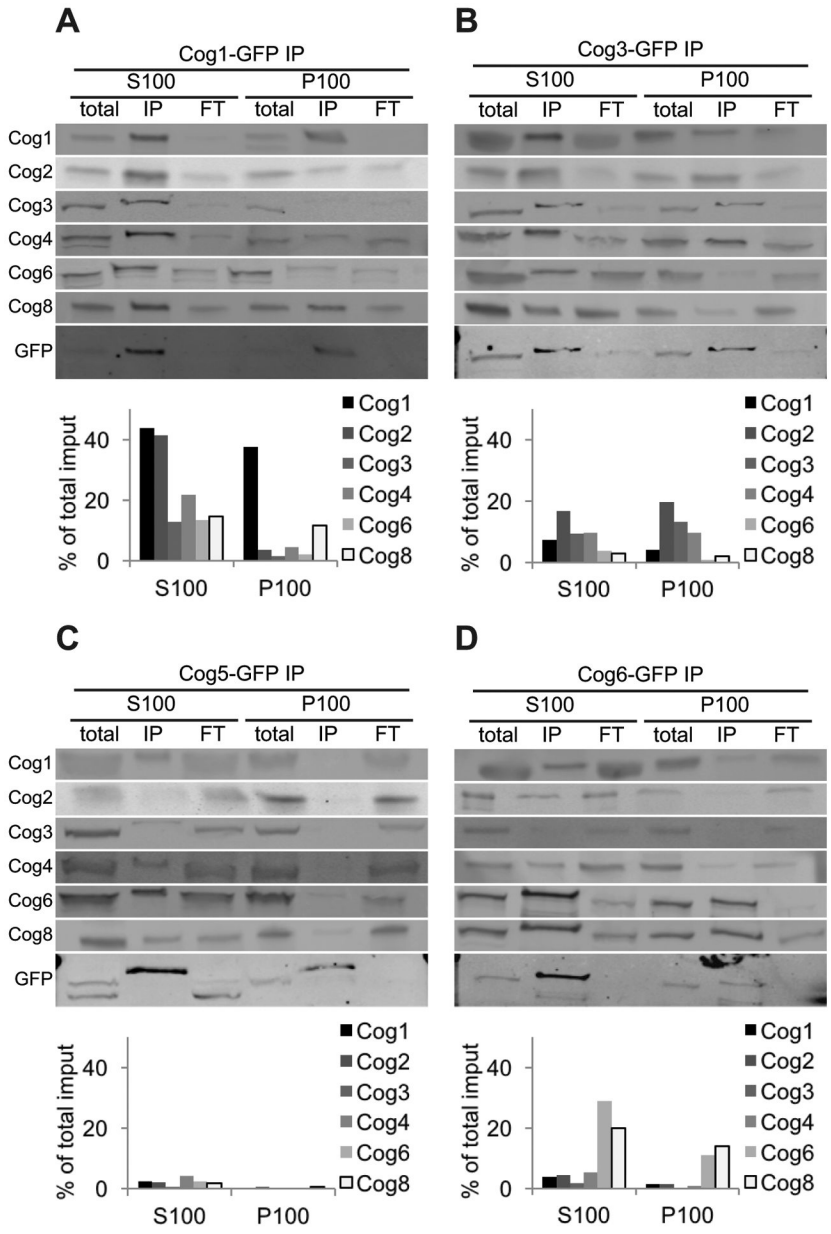

Figure 1.

Interactions of COG subunits. Lysates from cells expressing Cog1-GFP (A), Cog3-GFP (B), Cog5-GFP (C) or Cog6-GFP (D) were separated into S100 (cytosol) and P100 (membrane) fractions by centrifugation at 100,000 × g. S100 and P100 fractions were immunoprecipitated (IP) with anti-GFP. IP and 10% immunodepleted/flow-through (FT) fractions were separated by SDS-PAGE and blotted with antibodies against Cog1–8. 10% input of solubilized proteins was run as a control. The bottom bar graph shows IP efficiency of upper blots. IP efficiency values were calculated by dividing IP by input.

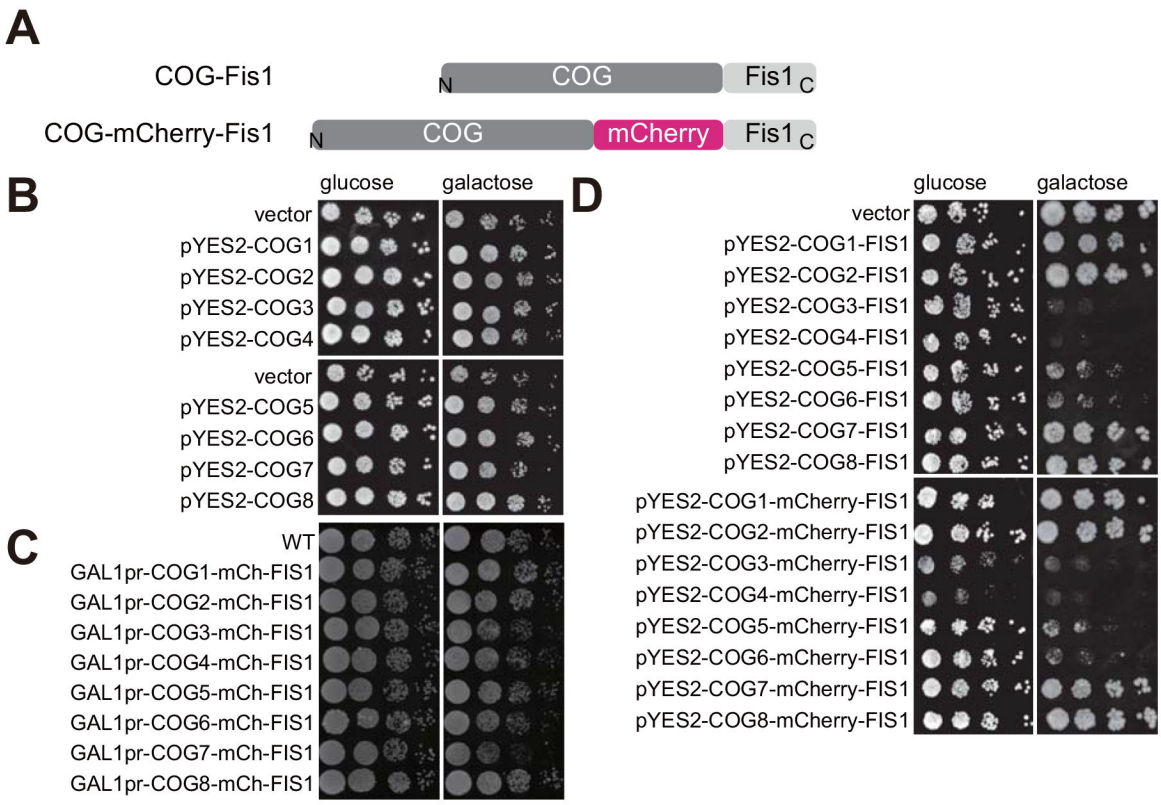

Figure 2.

Growth of COG-mCherry-Fis1 expressing cells. (A) COG-Fis1 and COG-mCherry-Fis1 fusions. (B) COGs were expressed under *GAL1* promoter by multi copy plasmids. Cells were grown on synthetic minus uracil plates containing 2% glucose or 2% galactose at 30˚C. (C) COG-mCherry-Fis1s were expressed under *GAL1* promoter by plasmids integrated into chromosome. Cells were grown on YP plate containing 2% glucose or 2% galactose at 30˚C. (D) COG-Fis1s or COG-mCherry-Fis1s were expressed under *GAL1* promoter by multi copy plasmids. Cells were grown on synthetic minus uracil plates containing 2% glucose or 2% galactose at 30˚C.

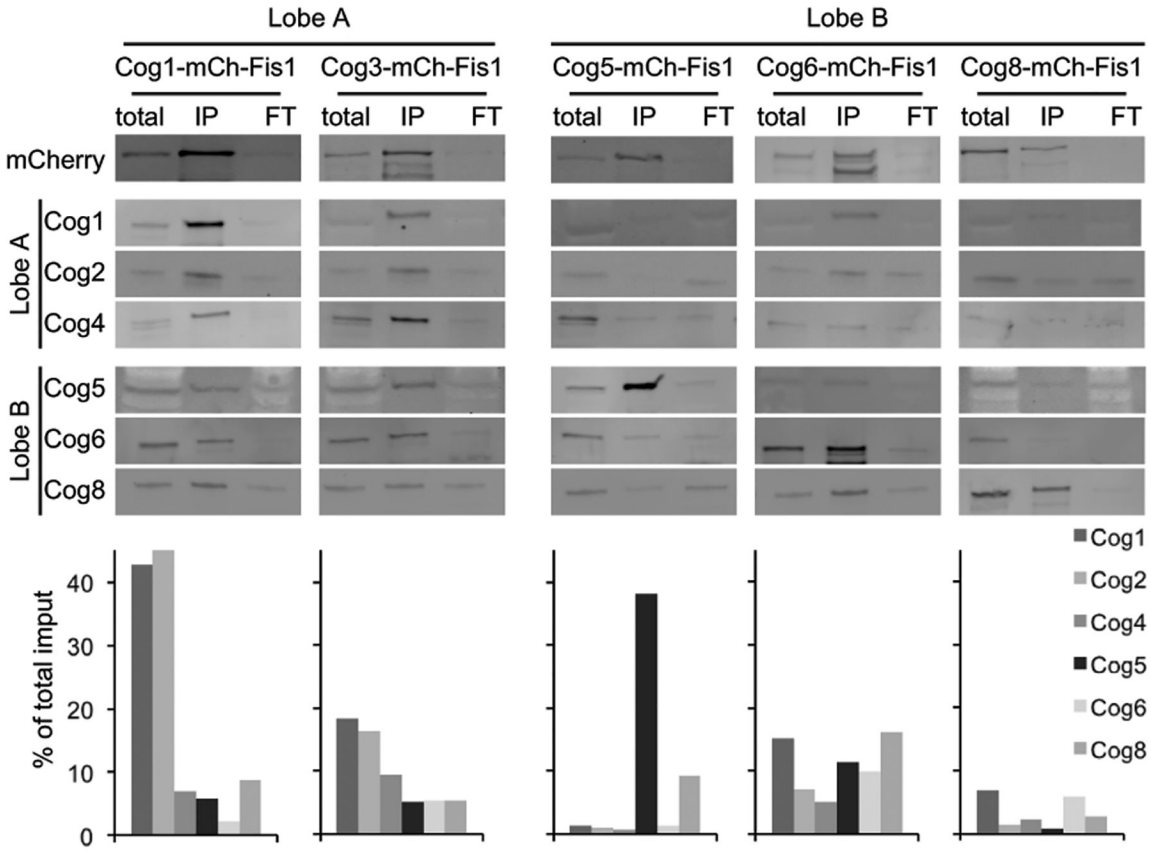

Figure 3.

COG-mCherry-Fis1 recruited other subunits to the mitochondria. COG-mCherry-Fis1s were expressed under *GAL1* promoter by plasmids integrated into chromosome. Yeast cell lysates were immunoprecipitated (IP) with mCherry-Nanobody beads. IP and 5% immunodepleted/flow-through (FT) fractions were separated by SDS-PAGE and blotted with antibodies against mCherry, Cog1, 2, 4, 5, 6 and 8. 5% input of yeast total lysate was run as a control. The bottom bar graph shows IP efficiency of upper blots. IP efficiency values were calculated by dividing IP by input.

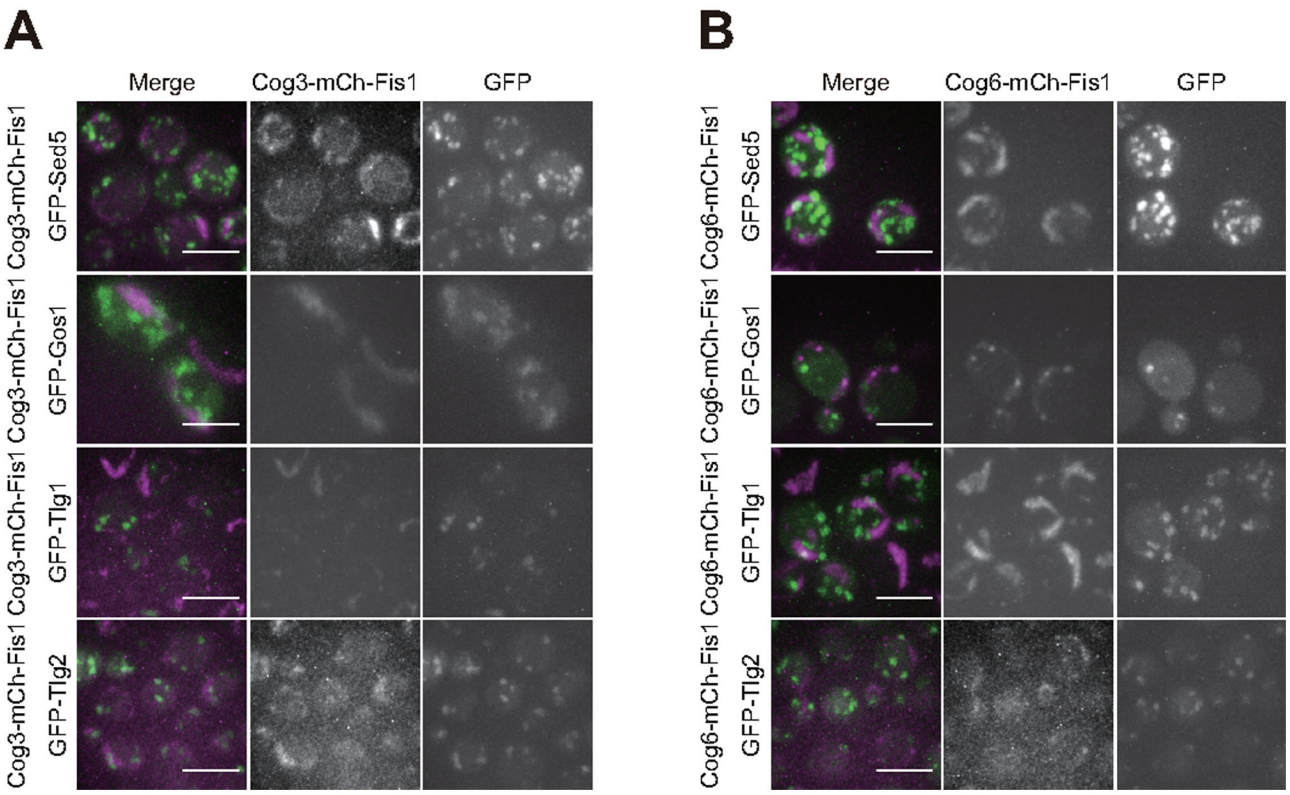

Figure 4.

Observation of Cog3- and Cog6-mCherry-Fis1 and SNARE proteins. (A) Cog3-mCherry-Fis1 and (B) Cog6-mCherry-Fis1 were expressed under *GAL1* promoter by plasmids integrated into chromosome. GFP tagged SNARE proteins, Sed5, Gos1, Tlg1 and Tlg2 were constitutively expressed by low copy plasmids. Cells were grown in synthetic medium containing 1% raffinose overnight, then in synthetic medium containing 2% galactose for 3 h at 30˚C and observed by SCLIM. Maximum intensity projections were shown. Scale bar, 5 μm.